Article

Trimorphism of a binary cocrystal system with hydrogen-bonded zig-zag, double helix and quadruple helix structures

Check for updates

Andrew J. E. Duncan[1], Celymar Ortiz-de León[1], María G. Vasquez-Ríos [2], Dale C. Swenson[1] & Leonard R. MacGillivray [1,2] ✉

Helices are present in the most important biomolecules (i.e., RNA, DNA). Helices are formed in biology and the laboratory using subunits with information encoded based on molecular recognition. The production of abiotic helical structures is an ongoing goal in synthetic and materials chemistry and has involved the development of organic and metal-organic materials that rely on complementarity of noncovalent forces (e.g. hydrogen bonds, coordination bonds) for helix formation. Herein, we describe a series of supramolecular isomers of three hydrogen-bonded organic cocrystals involving components that self-assemble and show progression at the structural level from a zig-zag chain to a double helix and to a quadruple helix. The isomers constitute a form of trimorphism involving a binary cocrystal system and we show that the polymeric structures can be interconverted through solvent-mediated phase transformations. We demonstrate the cocrystal involving the double helix to possess components that undergo an intermolecular [2 + 2] photodimerization in the crystalline state.

Of the common architectures in biological systems, helices (e.g., RNA, DNA) are of fundamental importance (e.g., relay chemical information)[1,2]. Ribonucleic acid (RNA) and deoxyribonucleic acid (DNA) are single- and double-stranded helices, respectively, with the components assembling through hydrogen bonds. Mathematically, the three-dimensional (3D) structure of a helix is derived from the 2D structure of a zig-zag[3]. The structures of zig-zags and helices are, more generally, examples of skew apeirogons, which are part of a class of infinite 2-polytopes with vertices that are not all colinear (Scheme 1). Progression of the structure of a zig-zag to a helix requires addition of an axis of rotation wherein the vertices are located to lie on the surface of a cylinder[3].

In this report, we describe a binary cocrystal with components that self-assemble to progress at the structural level from a zig-zag to a double helix and to a quadruple helix (Scheme 2). The formation of the 1D structures, which are related as supramolecular isomers[4], is manifested as three crystal polymorphs (**Forms I-III**), wherein the components of each trimorph self-assemble through hydrogen bonds. We show the generation of the polymorphs to be influenced by water, with solutions of higher water content promoting the formation of the quadruple helix. We also show mechanochemistry and heat to promote the formation of the double helix and quadruple helix, respectively. While the development of self-assembled zig-zags and helices being ongoing challenges in synthetic chemistry (e.g., catalysis) and materials sciences (e.g., optoelectronics)[5,6], we are unaware of a

case wherein the components of a purely organic multi-component system, such as a cocrystal, self-assemble to generate zig-zag and helical structures. Related solids composed of metal-organic components, which are sustained by coordination bonds, are reported to form zig-zags and helices in limited cases[6].

Results and Discussion

The binary cocrystal (**f-cat**)·(**bpe**) (where: **f-cat** = 3-fluorocatechol; **bpe** = *trans*-1,2-bis(4-pyridyl)ethylene) is trimorphic[7]. Each trimorph is obtained through solution-mediated phase transformation[8]. Specifically, each form is generated from a slightly opened screw-top sample vial involving an equimolar solution of **f-cat** (42 mg) and **bpe** (60 mg) in methanol/water (4 mL, 1:1). **Form I** (yellow plates) is generated in a period of 5 min upon precipitation from a resulting orange solution. **Form II** (orange-green dichroic prisms) is generated in the same solvent system after a period of 10 h from a green solution. Prolonged suspension of **Form II** for 20 h results in the generation of **Form III** (blue needles) from a blue solution.

As chemical building blocks, **f-cat** and **bpe** can function as double hydrogen-bond donors and acceptors, respectively. The diol **f-cat** can furthermore adopt one of nine likely conformations to support a self-assembly process with **bpe** (Scheme 3).

[1]Department of Chemistry, University of Iowa, Iowa City, IA, USA. [2]Département de Chimie, Université de Sherbrooke, Sherbrooke, QC, Canada. ✉e-mail: Leonard.MacGillivray@USherbrooke.ca

Self-assembly of trimorphs

Single-crystal X-ray diffraction (SCXRD) analysis reveals the components of **Form I** to crystallize in the chiral orthorhombic space group $P2_12_12_1$ with two molecules each of **f-cat** and **bpe** in the asymmetric unit (Fig. 1). The components form a 1D zig-zag chain along a 2_1-screw with the **f-cat** molecules adopting a *gauche-syn* conformation (Fig. 1a,b) (Table 1). The chains involve two unique (**f-cat**)·(**bpe**) units within the zig-zag chain based on a repeat distance slightly under 2.0 nm (19.6 Å). The components are sustained by O-H···N hydrogen bonds [O···N distances (Å): O(1)···N(1) 2.701(9)/O(3)···N(2) 2.698(9) and O(4)···N(3) 2.762(9)/O(2)···N(4) 2.823(10)]. The chains interdigitate to exhibit a tongue-in-groove fit within the crystallographic *bc*-plane (Fig. 1c).

In principle, the hydrogen bonding of the zig-zag chain can be manifested as two supramolecular isomers[7] wherein the F-atoms point either in the same (parallel) or opposite (antiparallel) directions within an individual chain. For **Form I**, the **f-cat** components point in opposite directions, interacting with two crystallographically distinct **bpe** molecules. The shortest hydrogen-bond distances involve the more acidic hydroxyl group adjacent to the F-atom, with the components of the chain twisted (twist angles: 6.7°, 25.6°, 13.9°, 12.3°) about each hydrogen bond.

In contrast to **Form I**, the components of **Form II** self-assemble to form a double helix (Fig. 2). The components crystallize in the monoclinic centrosymmetric space group C2/c with one molecule each of **f-cat** and **bpe** in the asymmetric unit. As with **Form I**, the diol and bipyridine assemble via

O-H···N hydrogen bonds [O···N distances (Å): O(2)···N(1) 2.7623(2), O(1)···N(2) 2.7067(1)]. The self-assembly generates chains exhibit a longer overall repeat distance on the order of 3.0 nm (31.4 Å) compared to **Form I** (Fig. 2a, b), with **f-cat** adopting a *gauche-anti* conformation (hydroxyl group twist -130°).
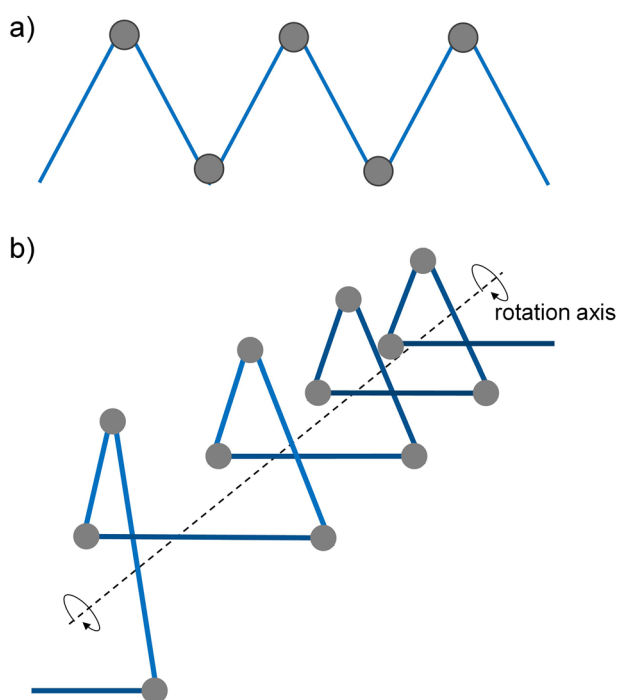
The F-atoms of **Form II**, in contrast to **Form I**, point in the same direction (Fig. 2a) along each helix chain, with the helixes running along a crystallographic *b*-glide plane in a head-to-head arrangement. The components of each strand are more twisted (twist angles: 80.3° and 73.9°) about each hydrogen bond compared to **Form I**. Offset infinite and face-to-face π-π stacking of **bpe** [centroid···centroid (Å): 3.867(5)] results in adjacent double helices related by a crystallographic center of inversion (Fig. 2c). The close packing is also mediated by edge-to-face π-interactions of the pyridyl groups and **f-cat**.

Whereas the components of **Form I** and **Form II** form a zig-zag and double helix, respectively, the components of **Form III** self-assemble to form a quadruple helix. The components crystallize in the trigonal space group $R\bar{3}$ with one molecule of **f-cat** and **bpe** in the asymmetric unit. As with **Form I** and **II**, the components generate 1D chains sustained by O-H···N hydrogen bonds [O···N distances (Å): O(1)···N(1) 2.692(1), O(2)···N(2) 2.708(1)] (Fig. 3). The chains participate, in contrast to **Form II**, as a quadruple helix along the crystallographic *c*-axis wherein the **f-cat** molecules adopt an *anti-anti* conformation. As with **Form II**, the F-atoms of **Form III** point in the same direction within a chain (Fig. 3a), with the helices oriented in a head-to-head arrangement. The helical chains tessellate within the *ab*-plane with packing based on triangles with neighboring helices being of opposite handedness. The F-atoms of the helices converge with F···F interactions at a core separated by 3.820(2) Å. Each helical chain exhibits an overall repeat distance larger than **Forms I** and **II**, being on the order of 5.0 nm (48.2 Å) and with the components also twisted (36.8° and 13.3°) from coplanarity.
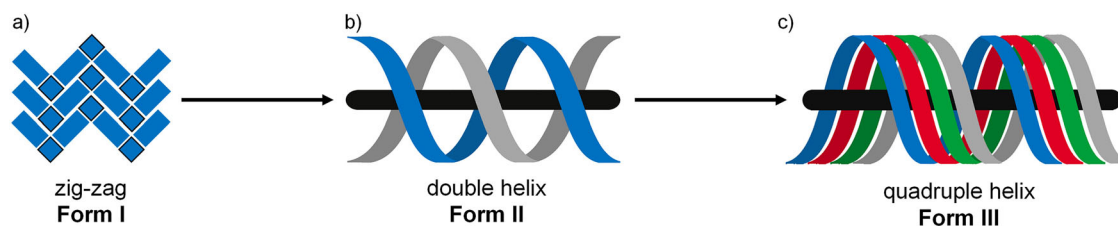
Role of solvent

To further elucidate the role of solvent in supporting the formation of the polymorphs, we have determined that when equimolar **f-cat** and **bpe** are dissolved in either methanol or water, the zig-zag **Form I** forms as a precipitate as single crystals and a powder. Prolonged suspension for a period of either 2 or 4 h results in a phase transformation to generate either the double helix **Form II** or quadruple helix **Form III**, respectively. **Form II** predominated in mixed solutions with at least 30% methanol (v:v) while **Form III** predominated in more aqueous solutions (Scheme 4). The dependence of **Form III** on the high-water content likely can be ascribed to a hydrophobic packing[9] effect involving the F-atoms that converge between the helices in the solid (Fig. 3d). A similar phenomenon has been described in materials composed of fluorinated proteins[10].

Form II was also determined to form by neat grinding, as well as liquid assisted grinding (LAG) with methanol[11]. When powder samples of either **Form I** or **Form III** were subjected to the grinding conditions, each solid converted to **Form II**. Grinding of a sample of **Form II** alone also did not result in a change in phase. A Hirshfeld analysis of each trimorph revealed C···C contacts to constitute the highest percentage in **Form II** (9.4%), which is consistent with the presence of the face-to-face π-stacks. Face-to-face stacking is significant in stabilizing the structures of proteins and other

a)

b)

rotation axis

Scheme 1 | Infinite skew apeirogons. **a** zig-zag skew and **b** helical polygon.

a)   b)   c)

zig-zag   double helix   quadruple helix
Form I   **Form II**   **Form III**

Scheme 2 | Supramolecular isomers as crystal polymorphs. **a** zig-zag, **b** double helix, and, **c** quadruple helix. Rotation axes for Forms II and III as black horizontal lines.

Scheme 3 | Conformations of f-cat (present study highlighted in blue).

syn-syn

syn-anti

syn-gauche

anti-anti

anti-syn

anti-gauche

gauche-gauche
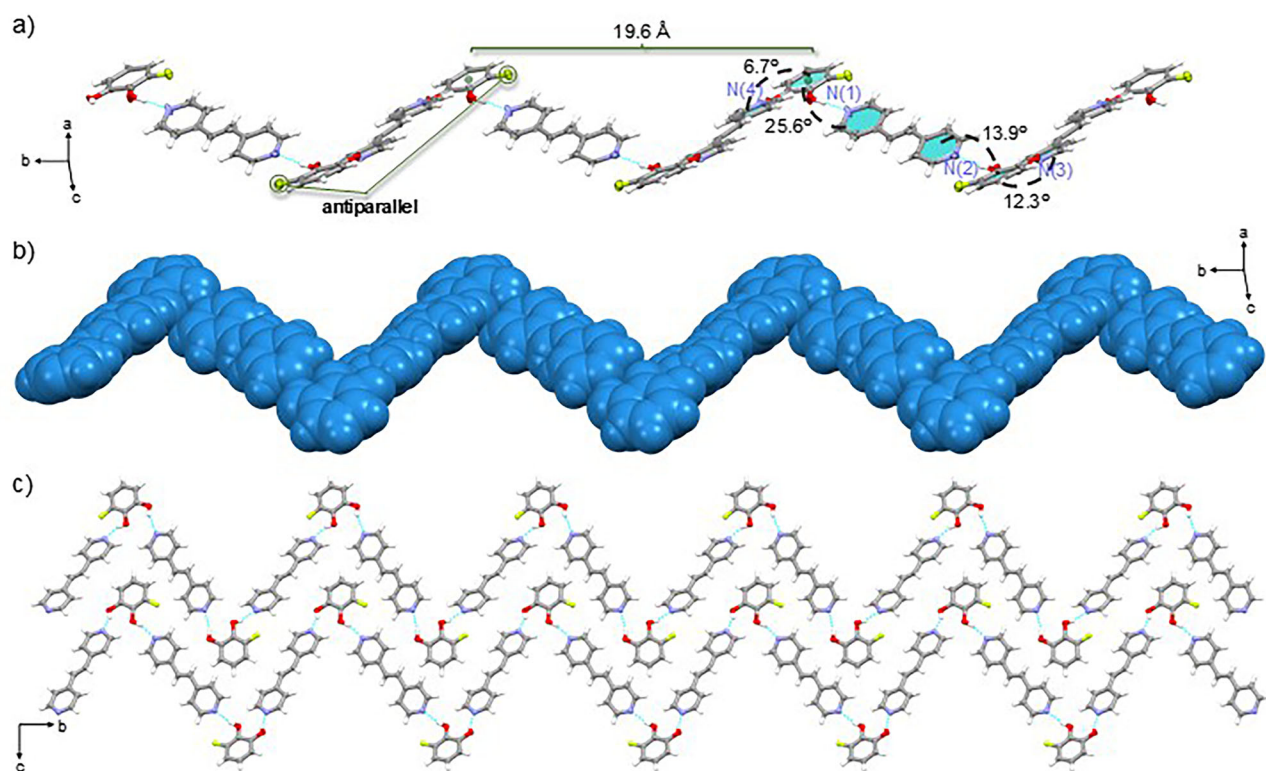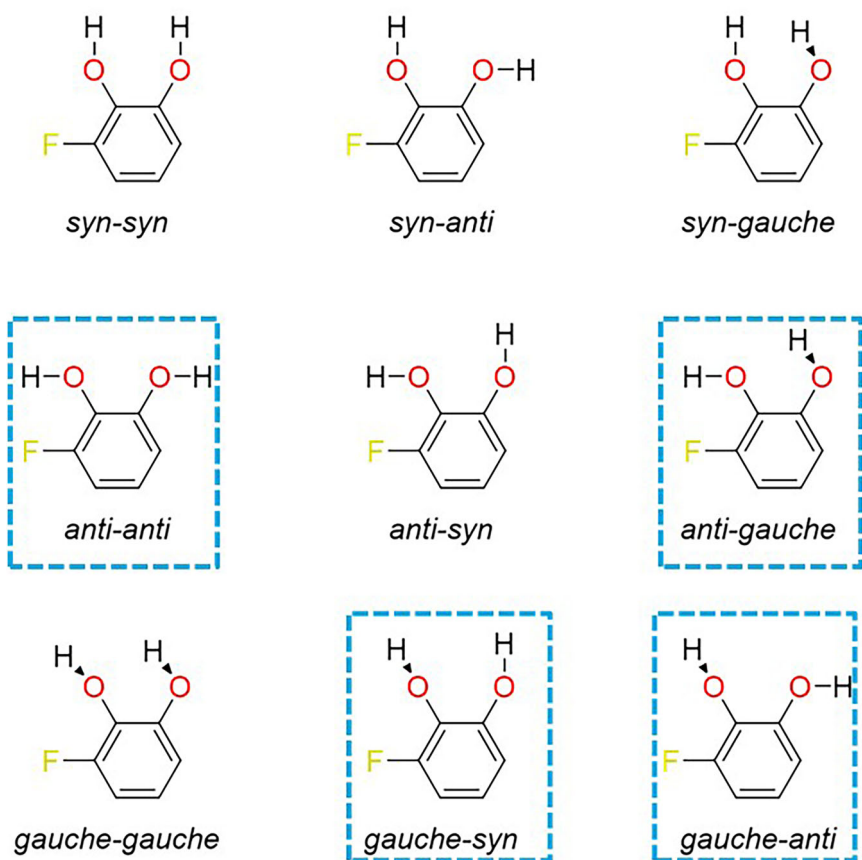
gauche-syn

gauche-anti

Fig. 1 | X-ray structure Form I. a zig-zag chain, **b** space-filling of single chain, and **c** packing of zig-zags.

biomolecules[9]. The stability of **Form II** can be attributed to the presence of the face-to-face π-stacks. The prevalence of the stacking is corroborated with energy framework calculations at the B3LYP/6-311 G(d,p) level using CrystalExplorer where the packing of **Form II** involves dominant dispersion energies (Supplementary Fig. 5). We note that heating of a separate sample of **Form II** at 130 °C for 2 h resulted in a phase transformation to **Form III** (Supplementary Fig. 3).

Photoreactivity of π-stacks of double helix

The proximity of the C=C bonds (3.675(4) Å) within the stacks and between the double helices of **Form II** renders the solid photoactive[12–14]. Specifically, when **Form II** was subjected to UV-radiation (72 h), the C=C bonds of **bpe** underwent an intermolecular $[2 + 2]$ photodimerization to afford *rctt*-tetrakis(4-pyridyl)cyclobutane (**tpcb**) stereospecifically and in near quantitative yield. The generation of **tpcb** was evidenced by the complete disappearance of the alkene peak at 7.65 ppm and appearance of the cyclobutane peak at 4.70 ppm on the ^{1}H NMR spectrum (Supplementary Figs. 7 and 8).

Table 1 | Structural parameters for 1D chains of polymorphs

polymorph	Form I	Form II	Form III
topology	zig-zag	double helix	quadruple helix
f-cat conformation	*gauche-syn*	*gauche-anti*	*anti-anti*
f-cat directionality	antiparallel	parallel	parallel
repeat length (Å)	19.6	31.5	48.2

When the resulting photoreacted solid was dissolved in ethanol, single crystals as colorless plates of composition 2(**f-cat**)·(**tpcb**) formed. The asymmetric unit consists of one full molecule of **tpcb** and two molecules of **f-cat**, which crystallize in the monoclinic space group $P2_1/c$ (Fig. 4). The components generate a O-H···N hydrogen-bonded corrugated network within the crystallography *ab*-plane [O···N distances (Å): O(1)···N(3) 2.682(2), O(2)···N(4) 2.694(2), O(3 A)···N(2) 2.661(2), O(4 A)···N(1) 2.592(2)] (Fig. 4a). The cyclobutanes of 2(**f-cat**)·(**tpcb**) are bridged by **f-cat** in *anti-gauche* (-175.75°) and *gauche-anti* conformations (177.7°) (Fig. 4b, c). The network can be simplified as a **sql** topology (point symbol $4^4.6^2$) with the nodes as the centroids of the cyclobutane rings of **tpcb** (Fig. 4d)[15]. Thus, the photodimerization supports a change from a double helix to a **sql** network. While $[2 + 2]$ photodimerizations in the solid state have been reported between 3D network structures (i.e., diamondoid networks)[16], we are unaware of an example wherein an intermolecular photodimerization occurs between helical structures.

Conclusions

In this report, we have described trimorphism involving a hydrogen-bonded binary cocrystal. With **f-cat** being unsymmetrical and conformationally flexible, supramolecular isomerism was expressed in **Form I** as a planar zig-zag and **Form II** and **Form III** as double and quadruple helices, respectively. Components of the double helices of **Form II** were also demonstrated to be photoactive in the solid state. We are now studying the scope of the polymorphism and extension to additional unsymmetrical coformers with the idea of determining the breadth of self-assembled frameworks that existence within the polymorphism domain. With the structures of zig-zags also being present in biochemistry (e.g., Z-DNA), it is intriguing to consider whether
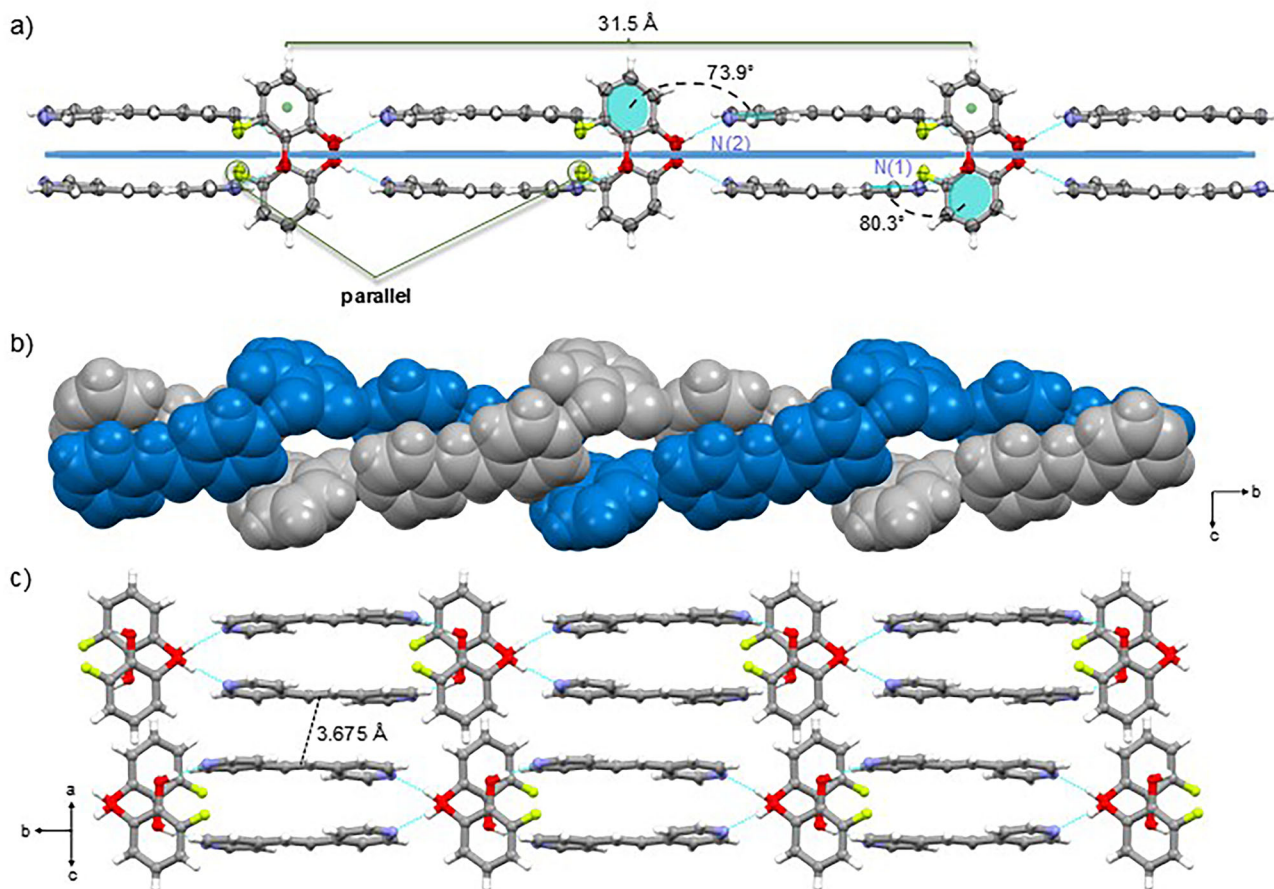

Fig. 2 | X-ray structure of Form II. a double helix, **b** space-filling of double helix, and **c** packing of neighboring helices.
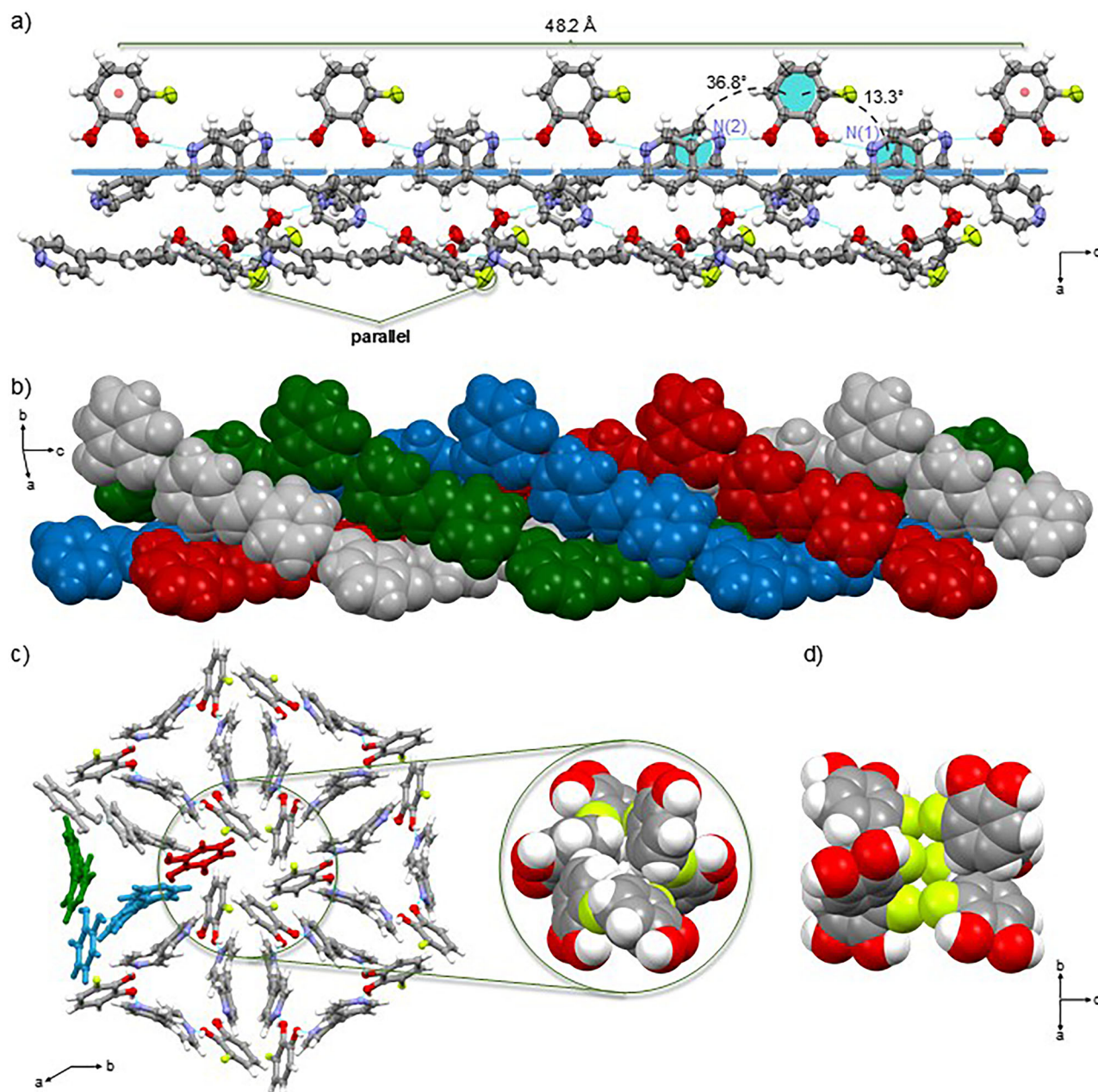
Fig. 3 | X-ray structure Form III. a quadruple helix, **b** space-filling of showing intertwined hydrogen-bonded chains, **c** hexagonal packing of neighboring quadruple helices with highlight of F-atoms, and **d** isolated cluster of F-atoms (inset, space-filling).

zig-zags of biological origin have a capacity to spontaneously evolve and self-assemble into helical structures.

Materials and Methods

Materials

3-fluorocatechol, acetonitrile, chloroform, ethyl acetate, and methanol were purchased from Sigma-Aldrich Chemicals. *Trans*-1,2-bis(4-pyridyl)ethylene was purchased from TCI Chemicals. All chemicals were used as received and without further purification.

Photodimerization experiments. A powder sample of **Form II** was subjected to UV-radiation (up to 72 h) using an ACE photocabinet equipped with an ACE quartz, 450 W, broadband, medium pressure, Hg-vapor lamp.

Nuclear magnetic resonance. Proton nuclear magnetic resonance (^{1}H-NMR) spectra were measured on a Bruker AVANCE 400 MHz spectrometer using DMSO-d_6 as the solvent.

Mechanochemistry. Liquid-assisted grinding (LAG) experiments were conducted in an FTS-1000 shaker mill using 5.0 mL PTFE jars and two stainless-steel balls (5.0 mm diameter). The reactions were performed at 20 Hz with 50 μL of solvent.

Single-crystal X-ray diffraction. Single-crystal X-ray diffraction (SCXRD) data were collected on a Bruker Nonius Kappa CCD single-crystal X-ray diffractometer using MoK$_\alpha$ radiation ($\lambda = 0.71073$ Å). Reflections were harvested from ϕ and ω scans with an intensity threshold of I > 2σ (I). Data collection, reduction, and cell refinement

Scheme 4 | Synthetic routes to each polymorph of (**f-cat**)·(**bpe**) cocrystal. Neat and liquid assisted grinding (50 μL of methanol) were subjected using a ball mill for up to 30 min.
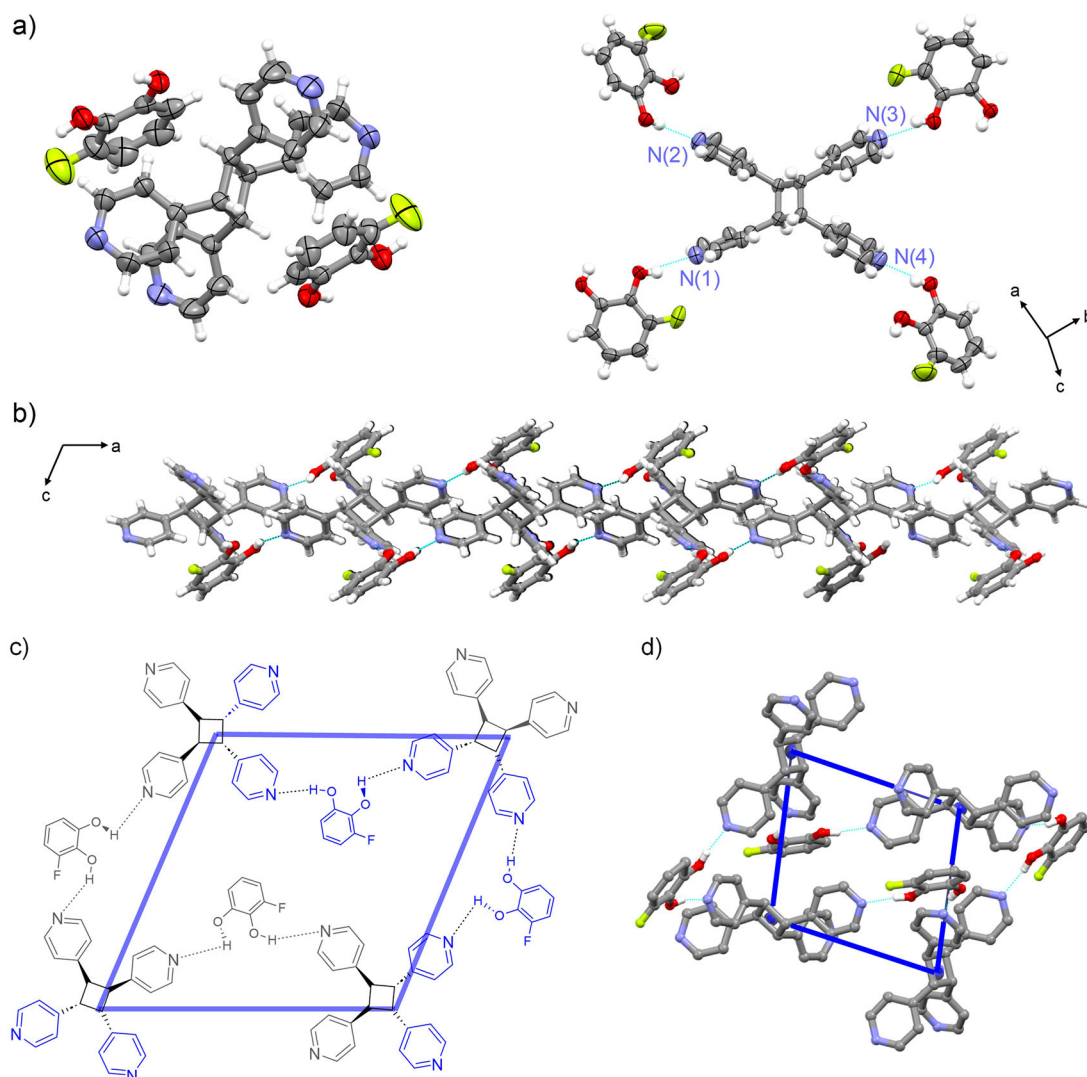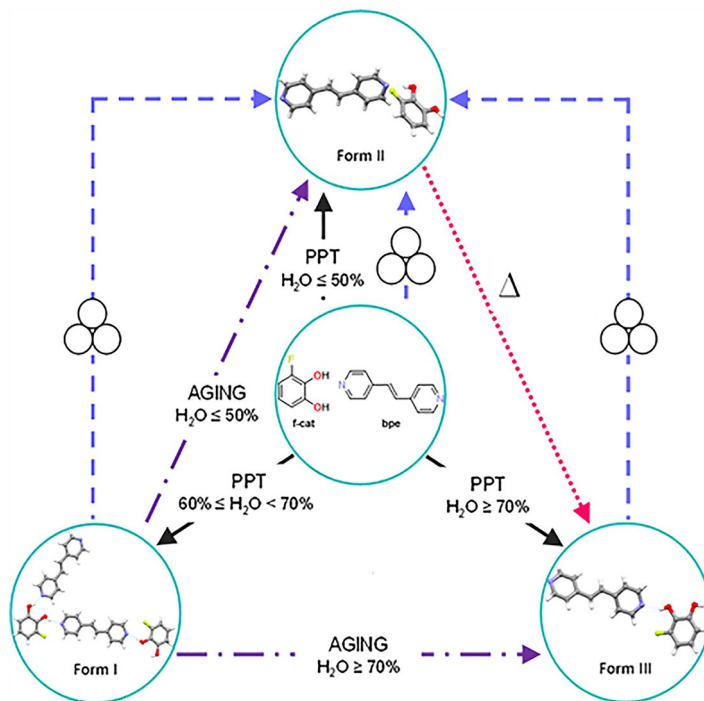

Fig. 4 | X-ray structure 2(f-cat)·(tpcb). a asymmetric unit, **b** hydrogen bonds, **c sql** topology, and **d** unit cell representation.

were accomplished using the Bruker Apex2 software suite. Using Olex2[17], structure solution and refinement were accomplished using SHELXT[18] and SHELXL[19], respectively. Non-hydrogen atoms were refined anisotropically. Hydrogen atoms of carbon atoms were refined in geometrically constrained positions.

Powder X-ray diffraction. Powder X-ray diffraction (PXRD) data were collected on a Bruker D8 Advance X-ray diffractometer using $CuK_{\alpha 1}$ radiation ($\lambda = 1.5418$ Å) in the range 5–45° (scan type: coupled Two Theta/Theta; scan mode: continuous PSD fast; step size: 0.019°) (40 kV and 30 mA).

Computational analysis. CrystalExplorer 21.5 program[20] was utilized to evaluate the interaction energies at B3LYP/6311 G(d,p) level. Interaction energies (E_{ele}, E_{mob}, E_{dis}, E_{rep}, E_{tot}) of **Forms I-III** are shown in Supplementary Table 4 and energy frameworks are illustrated in Supplementary Figs. 4–6.

Data availability
The data supporting this study is presented in the article and its supplementary information. The X-ray crystallographic data for structures reported in this Article have been deposited at the Cambridge Crystallographic Data Centre (CCDC), under deposition numbers CCDC 2431180, 2431183, 2431185, and 2431187. These data can be obtained free of charge from The Cambridge Crystallographic Data Centre via www.ccdc.cam.ac.uk/data_request/cif.

References
1. Banfalvi, G. Structural organization of DNA. *Biochem. Educ.* **14**, 50–59 (1986).
2. Ghosh, A. & Bansal, M. A glossary of DNA structures from A to Z. *Acta Crystallogr. D.* **59**, 620–626 (2003).
3. Coexeter, H. S. M. Regular Complex Polytopes (London: Cambridge University Press, 1974).
4. Hennigar, T. L., MacQuarrie, D. C., Losier, P., Rogers, R. D. & Zaworotko, M. J. Supramolecular isomerism in coordination polymers: conformational freedom of ligands in [Co(NO$_3$)$_2$(1,2-bis(4-pyridyl)ethane)$_{1.5}$]$_n$. *Angew. Chem. Int. Ed. Engl.* **36**, 972–973 (1997).
5. Yashima, E. et al. Supramolecular helical systems: helical assemblies of small molecules, foldamers, and polymers with chiral amplification and their functions. *Chem. Rev.* **116**, 13752–13990 (2016).
6. Zhang, J.-P., Huang, X.-C. & Chen, X.-M. Supramolecular isomerism in coordination polymers. *Chem. Soc. Rev.* **38**, 2385–2396 (2009).
7. Ortiz-de León, C. & MacGillivray, L. R. Clues from cocrystals: a ternary solid, polymorphism, and rare supramolecular isomerism involving resveratrol and 5-fluorouracil. *Chem. Commun.* **57**, 3809–3811 (2021).
8. Yu, J., Henry, R. F. & Zhang, G. G. Z. Cocrystal screening in minutes by solution-mediated phase transformation (SMPT): preparation and characterization of ketoconazole cocrystals with nine aliphatic dicarboxylic acids. *J. Pharm. Sci.* **114**, 592–598 (2025).
9. Dalvi, V. H. & Rossky, P. J. Molecular origins of fluorocarbon hydrophobicity. *Proc. Natl. Acad. Sci. USA* **107**, 13603–136067 (2010).
10. Marsh, E. N. G. Fluorinated proteins: from design and synthesis to structure and Stability. *Acc. Chem. Res.* **47**, 2878–2886 (2014).
11. Karki, S., Friscic, T., Jones, W. D. & Motherwell, S. Screening for Pharmaceutical Cocrystal Hydrates via Neat and Liquid-Assisted Grinding. *Mol. Pharm.* **4**, 347–354 (2007).
12. MacGillivray, L. R. et al. Supramolecular control of reactivity in the solid state: from templates to ladderanes to metal-organic frameworks. *Acc. Chem. Res.* **41**, 280–291 (2008).
13. Hutchins, K. M., Sumrak, J. C., Swenson, D. C. & MacGillivray, L. R. Head-to-tail photodimerization of a thiophene in a co-crystal and a rare adipic acid dimer in the presence of a heterosynthon. *CrystEngComm* **16**, 5762–5764 (2014).
14. Paul, A. K., Karthik, R. & Natarajan, S. Synthesis, structure, photochemical [2 + 2] cycloaddition, transformation, and photocatalytic studies in a family of inorganic organic hybrid cadmium thiosulfate compounds. *Cryst. Growth Des.* **11**, 5741–5749 (2011).
15. Mitina, T. G. & Blatov, V. A. Topology of 2-periodic coordination networks: toward expert systems in crystal design. *Cryst. Growth Des.* **13**, 1655–1664 (2013).
16. Park, I.-H. et al. Metal–organic organopolymeric hybrid framework by reversible [2+2] cycloaddition reaction. *Angew. Chem. Int. Ed.* **53**, 414–419 (2014).
17. Dolomanov, O. V. et al. OLEX2: A complete structure solution, refinement and analysis program. *J. Appl. Crystallogr.* **42**, 339–341 (2009).
18. Sheldrick, G. M. SHELXT: Integrated space-group and crystal structure determination. *Acta Crystallogr. Sect. Found. Adv.* **71**, 3–8 (2015).
19. Sheldrick, G. M. Crystal structure refinement with SHELXL. *Acta Crystallogr. C. Struct. Chem.* **71**, 3–8 (2015).
20. Spackman, P. R. et al. CrystalExplorer: A program for Hirshfeld surface analysis, visualization and quantitative analysis of molecular crystals. *J. Appl. Crystallogr.* **54**, 1006–1011 (2021).

Acknowledgements

Author contributions
A.J.E.D. designed the cocrystallization and carried out cocrystallization experiments, analyzed the results, and wrote the manuscript. C.O.-de L. carried out cocrystallization experiments, performed the photodimerizations, performed calculations, analyzed the results, and wrote the manuscript. M.G.V.-R. carried out cocrystallization experiments, performed calculations, and analyzed the results. D.C.S. collected the SCXRD data. L.R.M. supervised the research project and wrote the manuscript. All authors contributed to the discussion of the results.

Competing interests
The authors declare no competing interests.

Additional information
Supplementary information The online version contains supplementary material available at https://doi.org/10.1038/s42004-025-01856-w.

Correspondence and requests for materials should be addressed to Leonard R. MacGillivray.

Peer review information *Communications Chemistry* thanks Michael Ward and the other, anonymous reviewer(s) for their contribution to the peer review of this work.

Reprints and permissions information is available at http://www.nature.com/reprints